JOURNAL OF MATERIALS SCIENCE 37 (2002) 2997–3003

# Numerical modeling and experimental verification of mold filling and evolved gas pressure in lost foam casting process

Y. LIU, S. I. BAKHTIYAROV*, R. A. OVERFELT
*Solidification Design Center, 202 Ross Hall, Mechanical Engineering Department, Auburn University, AL 36849-5341, USA*

A simple mathematical model is developed to describe a lost foam casting process. Different aspects of the process, such as liquid metal flow, transient heat transfer, foam degradation and gas elimination were incorporated into this numerical model. Fluid velocity, temperature distribution within molten metal and pressure building-up in the mold cavity are predicted as a function of filling time and filling height. The model was verified by comparison of the predicted velocity profiles, temperature fields and back-pressures with the experimental data conducted in this work. Both coated and uncoated foam patterns were used in experimental part of this study. A good agreement between the predictions and the experimental data was found. 

## 1. Introduction

Lost foam casting is a much more complicated process in both physical and chemical aspects than traditional investment and sand mold casting. Many physical processes, such as heat and mass transfer, fluid flow, chemical reaction, solidification, etc. are involved in this casting technique. In addition, these phenomena occur within a very short period of time during the mold filling process. The most significant feature of the lost foam casting is the presence of solid expanded polymer foam in the path of the advancing molten metal front. As the molten metal fills the mold, the polymer foam undergoes complex transitions: collapse, melting, de-polymerization or ablation. The resulting by-products are either liquid or gaseous species. Researchers of lost foam casting process have been concerned with elimination of these degradation products, which are potential defect sources [1–3]. The gaseous degradation fragments may play a crucial role in mold filling and defect formation since the total volume of gaseous species is quite large (230 $cm^3/g$ at 750°C) [4], and all the liquid products must eventually be eliminated through refractory coating and sand in the form of gaseous species. Some researchers tried to measure back-pressure inside the mold as metal front advances. A gas pressure between 11 and 26 kPa in the mold was reported in iron casting [5]. Yang *et al.* [5] measured an evolved gas pressure in the mold for aluminum alloy casting. The obtained peak gas pressure values were in the range of 0.240 to 0.486 kPa, which is negligible compared to those in iron lost foam casting. The average velocity of molten aluminum during mold filling varied between 1.6 to 4.6 cm/s.

From experimental castings of aluminum alloy A356, Shih and Chang [6] determined that if the instantaneous filling velocity is less than 12.85 cm/s, a small amount of gasification occurred ahead of the advancing molten metal. At higher filling velocities a large amount of liquefied EPS was observed ahead of the metal front moving surface. From these results one would conclude that in aluminum lost foam casting, gas products are not generated, resulting in low pressure values [5].

The gas pressure, the melt velocity and the thickness of the gas layer were measured by Zhu *et al.* [7] during aluminum lost foam casting. For 27 cm melt head and 500 $\mu$m coating thickness they obtained an average filling velocity 2–4 cm/s and gas pressure 6.2–6.8 kPa.

Due to the complexity of the mathematical modeling of the lost foam process, most studies have been experimental in nature, although some semi-empirical formulations regarding the fluid flow and gaseous pressures generated from foam pattern degradation have been reported. The attempts on mathematical modeling of lost foam casting were scarce and highly limited to a few oversimplified calculations.

Tsai and Chen [8], Abayarathna and Tsai [9], and Abayarathna [10] used finite element method to solve the coupled heat and mass transport equations simultaneously. They employed this simulation technique for the following stages of the lost foam casting process:

- metal flow and heat transfer during the filling stage,
- the diffusion of carbon in the casting,
- heat and mass transfer in the sand mold.

However, the following major drawbacks existed in their model:

*Author to whom all correspondence should be addressed.

- some boundaries needed to be further refined,
- some crucial input data were not available at that time,
- there were no experimental results to compare with.

In a review paper, Ohnaka [11] proposed an algorithm, which considered the back pressure change due to the compression and gas flow through the vents and mold. Both mass and energy conservation equations were solved in a step-by-step manner.

Wang *et al*. [12] modified the existing computer program for simulation of conventional (empty mold) sand casting to simulate the fluid flow and heat transfer during mold filling and ensuing solidification for the lost foam casting processes in an arbitrary 3-D geometry. The momentum, heat and mass transport equations were solved using the finite difference method for metal flow interacting with the decomposing pattern, free surfaces, and refractory shell.

Up to now, no numerical model can be found which gives a quantitative prediction of the evolved gas pressure, and no experimental data are available to verify the existing models. The objective of this paper is to present a simple 1-D mathematical model which predicts the molten metal front velocity and back-pressure of the decomposed gases. We also present the results of an experimental study of the evolved gas pressure inside the mold as metal front advances and replaces EPS pattern which validated our numerical model.

## 2. Mathematical modeling

### 2.1. Physical model

For simplicity, we proposed one-dimensional model of lost foam casting. Fig. 1 is a schematic representation of the pattern cluster to be cast. Molten metal is poured from the pouring cup, which then flows through the hollow ceramic downsprue and horizontal runner system, and enters the casting. Once the molten metal is in contact with the foam pattern, the latter will be decomposed into liquid and gaseous products or their mixture, depending upon the metal temperature. We assume that in the gating system, metal is supposed to move in the same manner as in the conventional empty mold casting process. The maximum metal flow speed is reached at the bottom of downsprue, which is the speed of a free falling body. However, in the foam pattern part, the speed of the liquid metal flow is limited by the back-pressure which in turn depends on the polymer foam degradation rate as well as the rate of the gas escaping through refractory coating.

There are two coupled domains that have to be considered in the numerical modeling: molten metal and gas gap, which exists between metal front and solid foam pattern. These two domains are always varying their sizes during casting process. In addition, there might be a liquid layer existing close to the solid foam pattern, as reported in the literature. The speed of the liquid metal front is determined by the metallostatic head, fluid viscosity, flow path geometry, pattern material, pouring temperature, molding material, coating material and thickness, and etc. The temperature distribution also depends on the above parameters. Part of the heat is lost from metal surface directly into the coating and sand, but foam pattern is believed to be the biggest heat sink. The actual pattern decomposition rate is controlled by the heat transfer rate from the liquid metal front to a foam pattern. The internal gaseous pressure depends on the rate of gas generation as well as on the rate of gas escape. The former factor depends on the pattern density, casting-section thickness, and metal temperature, whereas the latter factor depends on the permeability of coating layer and sand mold, as well as on the available surface area for gases to escape. The size of gap between the metal front and the pattern depends on the dynamic balance of the pattern degradation rate, the rate of the gas escaping through the refractory coating, and the speed of the metal front.

From the above discussion, it is seen that there are so many parameters involved and they are coupled in lost foam casting process. It is impossible to simulate the whole process without any simplifications, whereas it is unacceptable if too many assumptions are made. Fig. 2 illustrates the mechanism and main parameters for the modeling. The following major assumptions are made in our formulation:

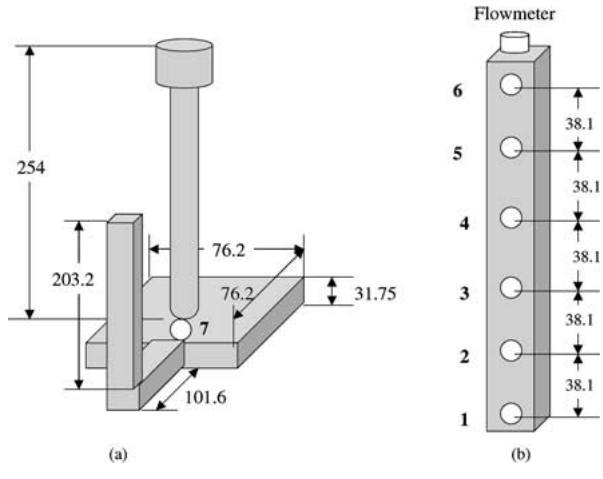


*Figure 1* Vertical cast pattern with downsprue and horizontal runner (a) and locations of temperature and pressure sensors (b). All sizes are in millimeters.

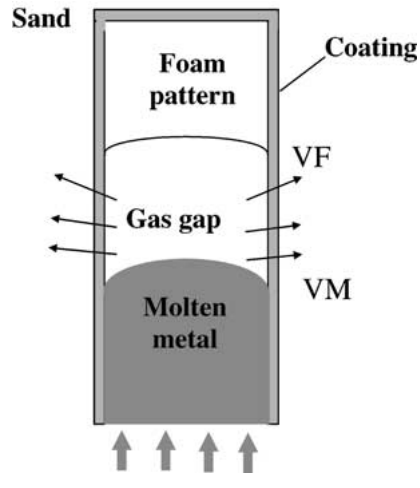


*Figure 2* Schematic representation of physical model.

- Metallostatic head is constant during the mold filling process
- Fluid flow and pattern degradation are one-dimensional
- Liquid metal is assumed non-viscous. This assumption is justified since pattern geometry is simple and a mold filling time is short
- The behavior of gaseous products follows an ideal gas law
- Gas flow through the coating obeys the Darcy's law (Reynolds numbers are low)
- The heat transfer coefficients are independent with temperature and time.

This model would allow predict the metal front velocity and pattern degradation rate as a functions of time, and estimating the evolved gas pressure.

## 2.2. Governing equations

The Bernoulli equation has been applied to the liquid metal flow:

$$\frac{P_0 - P_i}{\rho} + \frac{V_0^2}{2} - \frac{V_i^2}{2} + g(Y_0 - Y_i) + E_{fi} = 0, \quad (1)$$

where $P_0$ and $P_i$ are pressures on the metal front when it is at positions $Y_0$ and $Y_i$, respectively; $V_0$ and $V_i$ are mean velocities of the liquid metal front when it is at positions $Y_0$ and $Y_i$, respectively; $E_{fi}$ is the hydraulic energy losses when the liquid metal front moves from $Y_0$ to $Y_i$. The hydraulic energy losses term are function of the Reynolds number, and the configuration of the system between positions $Y_0$ and $Y_i$.

The heat transport equation was solved to obtain temperature distribution along $Y$ direction of foam pattern:

$$\frac{\partial T}{\partial t} = -V_m \frac{\partial T}{\partial Y} + \alpha \frac{\partial^2 T}{\partial Y^2}, \quad (2)$$

where $T$ is temperature, which is a function of time and position; $V_m$ is metal velocity in vertical direction (since the pattern had a uniform cross section, $V_m$ is not a function of position); $\alpha$ is the thermal conductivity of the liquid metal.

In order to obtain instant internal pressure $P_i$, gas domain was considered in each time step as:

$$P_i W_i = n_i R T, \quad (3)$$

where $W_i$ is the volume of gas domain at position $Y_i$; $n_i$ is mole number of the gas mixture; $R = 8.3144$ J/(mole K) is gas constant.

At any time or position, $n_i$ is determined by the gas generation and elimination. Heat flux $q$ at metal front was computed as:

$$q = -\alpha \frac{\partial T}{\partial Y}. \quad (4)$$

The part of the heat escapes through refractory coating, but the most of the heat passes through the gas domain and enters the solid foam pattern. The heat transfer mechanism might be very complicated, which probably involves heat conduction, convection and radiation. Here we simply use an equivalent heat transfer coefficient $H_f$, which equals to the foam degradation heat, and represents all these three factors. According to the data from the literature, EPS foam degradation heat is around 912 kJ/gram. This value was employed together with foam density and Equation 4 to determine the foam degradation velocity $V_f$.

$$V_f = \frac{q}{H_f \rho_f}, \quad (5)$$

where $\rho_f$ is the density of the EPS foam.

The gas elimination rate was calculated using Darcy's law:

$$q_g = \frac{\kappa}{v} \frac{dP}{dY}, \quad (6)$$

where $q_g$ is mass flux passing through the refractory coating, $k$ is coating permeability, $v$ is the gas viscosity, $dP$ is the pressure difference between the coating surfaces, and $dY$ is the coating thickness.

Once foam degradation velocity $V_f$ and metal moving velocity $V_m$ are computed, the gas volume, and then the gas pressure at any specific time is determined.

## 2.3. Numerical computation technique

The partial differential equations formulated above were solved together by finite difference method. Input and output data are determined at discrete points fixed in space and/or time. For Stefan-type problems, the moving boundary becomes a difficulty. In analytical solutions of the Stefan problem, the exact location of the interface is known explicitly, but in numerical solutions the position of the interface may only be determined if it resides on one of the discrete, pre-determined points (nodes). Usually, a coordinate transformation is used to 'fix' the moving interface. A "marker-and-cell" (MAC) technique, which puts small particles at the interface to identify it, was employed by the commercial casting software [13]. The most popular technique is a "volume of fraction" (VOF) technique, which uses "0" and "1" to identify empty and full nodes. Any node with a number between "0" and "1" is on the interface. These techniques are suitable for 3-D geometry. In the one-dimension problem the flat metal surface is assumed, and the position of metal front is simply a function of time.

Convection boundary conditions were assumed on the interfaces between the metal front/gas and the coating/environment domains. The boundary conditions used in our computations are:

$$V_m = 0 \quad \text{at} \quad Y = 0 \quad (7)$$

$$Y = 0, \quad \text{at} \quad t = 0 \quad (8)$$

$$P_0 = 101300\,\text{Pa}, \quad \text{at} \quad Y = 0 \quad (9)$$

$$k \frac{\partial T}{\partial Y} = h_f (T_i - T_\infty), \quad \text{at} \quad Y = Y_i, \quad t > 0 \quad (10)$$

$$k \frac{\partial T}{\partial L} = h_c (T_g - T_\infty), \quad \text{at} \quad Y = Y_i, \quad t > 0 \quad (11)$$

For a higher accuracy, a central finite-difference approximation was used to solve the discrete partial differential equations [14]. The boundary conditions were

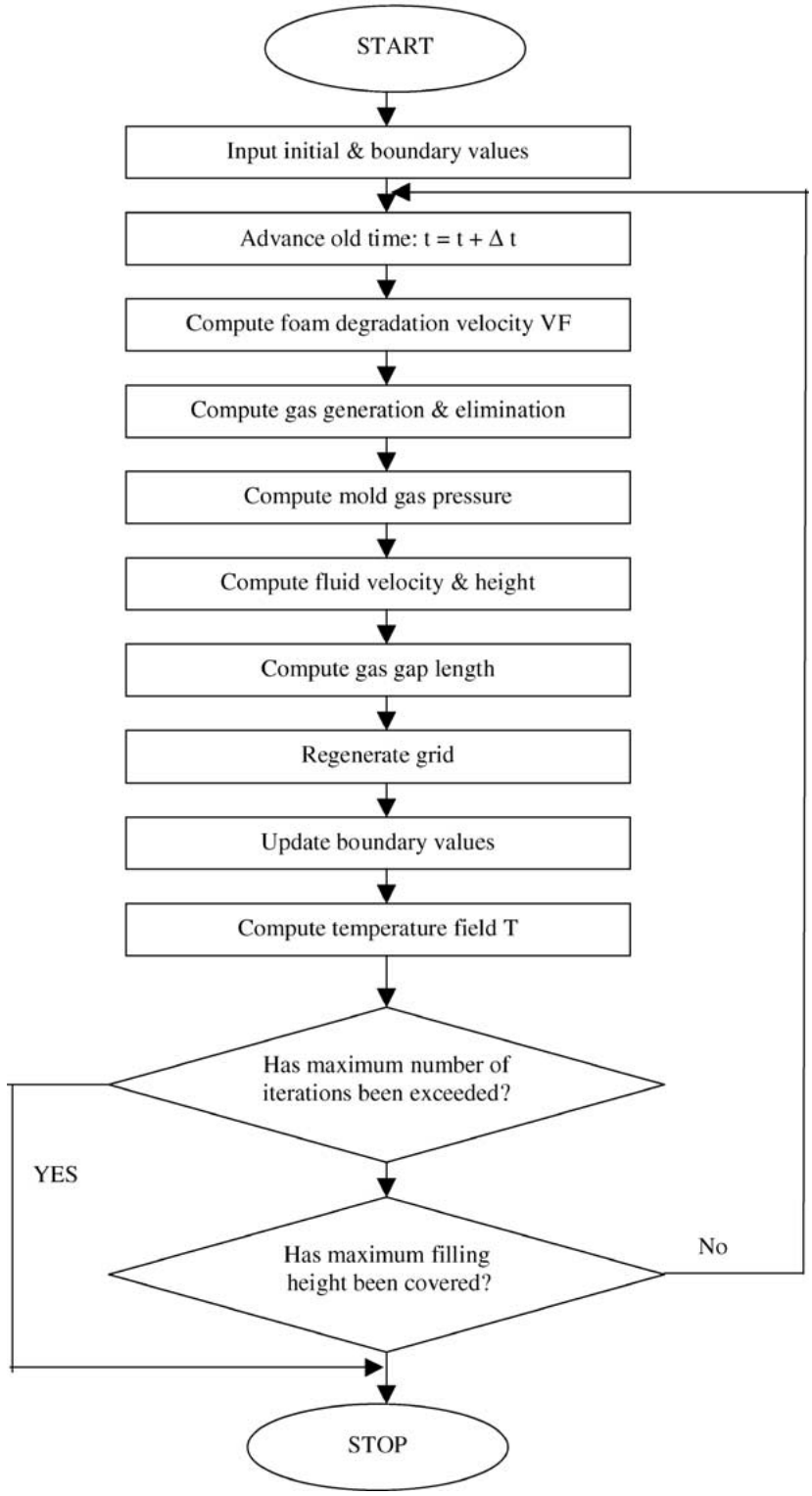


*Figure 3* Flow chart of LFCFLOW solution procedure.

also rewritten in second derivatives. The method of Crand-Nicolson was used to transform the partial differential equations into the implicit finite difference format. The resulting nonlinear algebraic equations were solved using Gauss-Seidel iteration. A second order accuracy was guaranteed by using above scheme.

The algorithm was programmed in Fortran 77 computing language. Fig. 3 shows a flow chart of the computations. Time step d$t$ was chosen to be $10^{-6}$ second, and distance step d$Y$ is 0.01 mm. For new iteration, the new values for metal front location, the temperature distribution in molten metal, the metal front velocity, the foam degradation speed, and the internal pressure were calculated based on the data from the last time step.

## 3. Experimental procedure

Experimental pattern was prepared according to Fig. 1. A 20 cm long bar was prepared using a hot wire cutter from a commercial EPS plate with a density of 0.025 g/cm$^3$. The pattern had a cross section area of 3.2 cm $\times$ 3.2 cm. The bead size of the EPS foam was

about 2 mm. Foam pattern was dipped into commercial refractory slurry and dried at a temperature of 40°C in a warm air stream overnight. The thickness of the coating was measured to be 0.5 mm after drying. A 30 cm height ceramic downsprue sited parallel to the pattern. In order to prevent any undesirable heat flux from the sprue onto the pattern during the filling process, the 10 cm horizontal runner was employed to connect the sprue and the pattern.

Starting from 0.64 cm from the bottom of the vertical foam pattern, six sets of thermocouples and bronze tubes (2 mm in diameter and 25 cm in length) were inserted into the foam pattern at the intervals of 3.8 cm apart. The other ends of the tubes were connected to the gas pressure transducers, which had the maximum range of 35 kPa. The pressure transducers were carefully calibrated in compressed air with the standard gas gauge. Both the temperature and pressure data were finally ported to the computer. Data were collected at the rate of 20 Hz. The whole data acquisition process lasted for more than three minutes to make sure that all the data for mold filling were collected.

The assembled pattern clusters were placed in a 46 cm diameter, 61 cm height steel flask. The flask was then filled with unbonded sand of 50 AFS grain fineness. In order to prevent spoiling the foam pattern by unexpected movement of gas tubes, sand was introduced into the flask and compacted manually to produce a closely packed mold.

A high frequency induction furnace was used to melt the alloy. The maximum capacity of the furnace was 20 kg of pure aluminum or 60 kg of iron. About 15 kg of aluminum alloy A319 was melted in our experiments. After melting, pure argon was introduced into the melt through a porous refractory media. The melt was purged continuously for 15 minutes and the temperature was adjusted to the desired pouring temperature. Then the metal was poured rapidly and in a single stream into the downsprue.

## 4. Results and discussion

The thermophysical properties of aluminum alloy A319 and casting conditions for the numerical calculations are summarized in Table I.

It is noted that although the $h_c$ and $h_b$ values used in the calculations are not obtained from actual experimental measurements, the results shown below are proved to be reasonable and sound. For comparison, two casting experiments were conducted. In first experiment the foam pattern was coated with a layer of refractory coating, which had a thickness of 0.5 mm, whereas the second test the pattern had no coating on the surface. Both the numerical modeling results and the experimental data were plotted in the same figures.

TABLE I Thermophysical properties of materials used and casting conditions

| Property | Symbol | Value |
|---|---|---|
| Liquid metal density | $\rho_m$ | 2340 kg/m$^3$ |
| Thermal conductivity of liquid metal | $\kappa$ | 304 W/(m K) |
| Specific heat of liquid metal | $c_v$ | 1180 J/(kg K) |
| Sand and solid foam temperature | $T_r$ | 298 K |
| Foam density | $\rho_f$ | 25 kg/m$^3$ |
| Foam degradation heat | $H_f$ | 912000 J/kg |
| Coating permeability | $k$ | 0.5E-11 m$^2$ |
| Gas viscosity | $v$ | 0.4E-4 kg/(m s) |
| Heat transfer coefficient to sand | $h_c$ | 1300 W/(m$^2$ K) |
| Heat transfer coefficient to gas | $h_g$ | 3300 W/(m$^2$ K) |
| Metal pouring temperature | $T_0$ | 1173.5 K, 1023 K |
| Metallostatic head | $Y_0$ | 0.35 m |

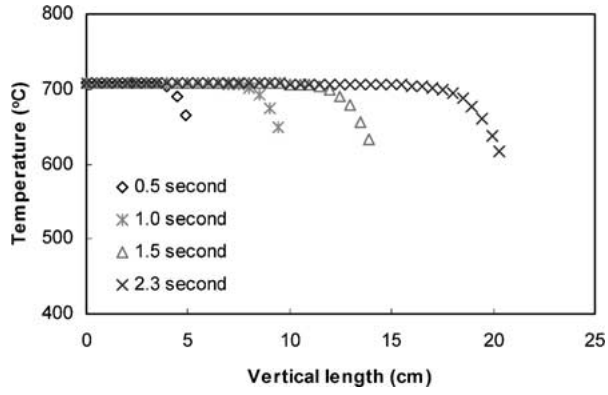


*Figure 4* Temperature distribution at different filling times (foam pattern without coating).

It is found that the numerically predicted profiles are in a good agreement with the experimental data. Fig. 4 shows temperature distributions along the vertical bar at different filling times. It took totally 2.3 seconds to fill up the pattern, which had the length of 20.3 cm. The temperature at the metal front was much lower than that at the other positions. This is due to the "quenching" effect of foam pattern degradation. As molten metal moved up, more and more heat was lost from metal front, which resulted in lower and lower metal front temperature. At the end of the mold filling process, the metal front temperature was dropped up to 617°C, whereas temperature at the gating point was still 709°C. For the complex geometry and big size patterns, fluidity of molten metal have to be considered. Casting defects such as folds are much easier to occur when two metal streams merge together.

Figs 5–7 show profiles for metal front position, velocity and temperature. Experimental data were recorded by the thermocouple response. It was noted that the mean metal flow speed is about 10 cm/s, which is much smaller than that in empty mold casting. In addition, no pressure was measured and predicted by the program. This indicates that for the castings without refractory coating, the foam pattern degradation occurs

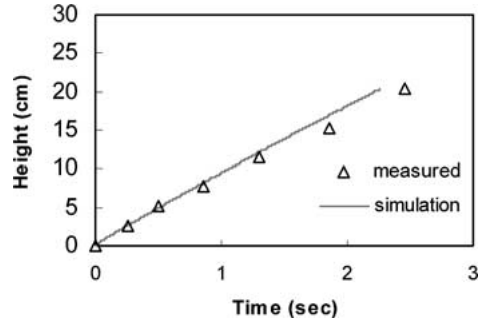


*Figure 5* Filling height as function of time (foam pattern without coating).

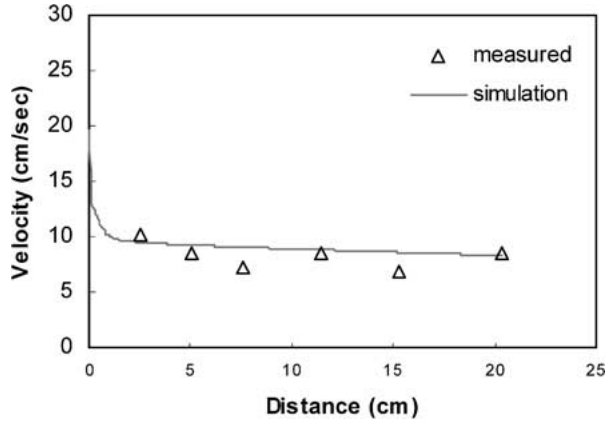


*Figure 6* Metal velocity profile (foam pattern without coating).

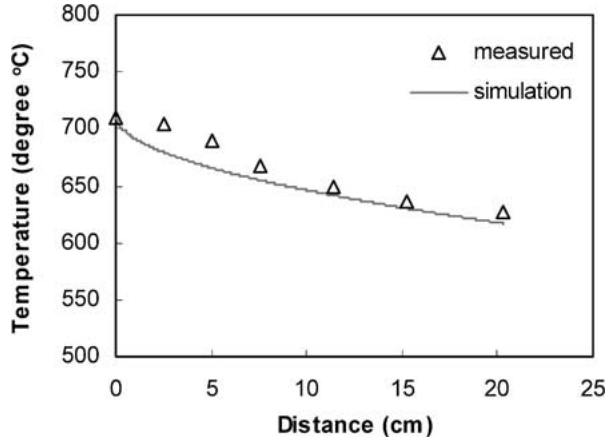


*Figure 7* Metal front temperature during mold filling process (foam pattern without coating).

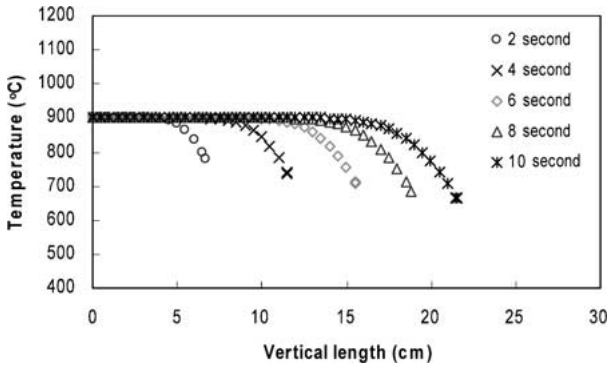


*Figure 8* Temperature distribution at different filling time (coated foam pattern).

instantly, and the resulting gaseous products are eliminated quickly.

The velocity, temperature and pressure profiles for the coated pattern castings are shown in Figs 8–12. It is evident from the Fig. 7, that the mold filling time was much longer than that for the uncoated pattern. More than 10 seconds was needed for metal to replace the foam pattern. Temperature losses at metal front exceeded 200°C. The temperature-dropping rate is 14°C/cm. If the heat loss through refractory coating is ignored, the temperature drop at the metal front due to the ablation of the foam pattern will be 490°C per 1 gram of the foam material. It is obvious that the degradation of the polymer at the metal front is highly

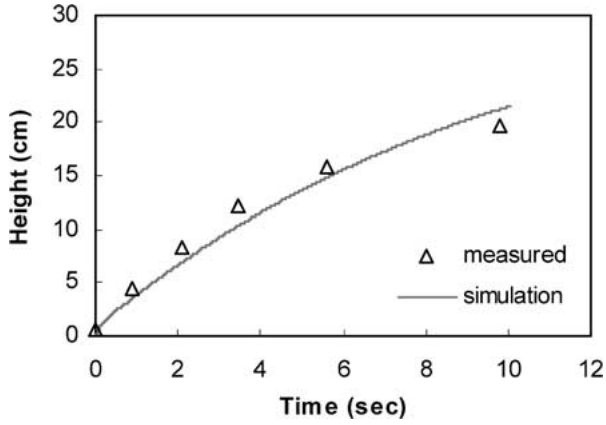


*Figure 9* Filling height as a function of time (coated foam pattern).

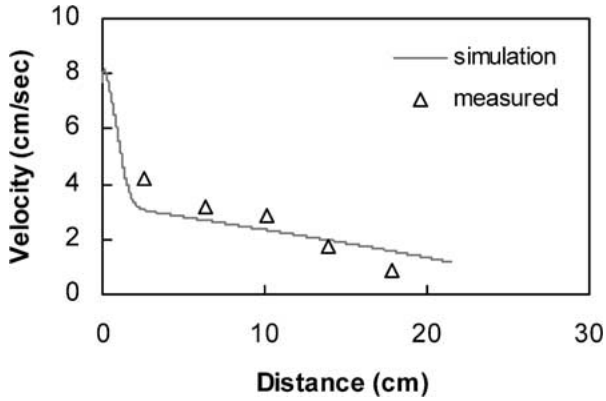


*Figure 10* Metal velocity profile (coated foam pattern).

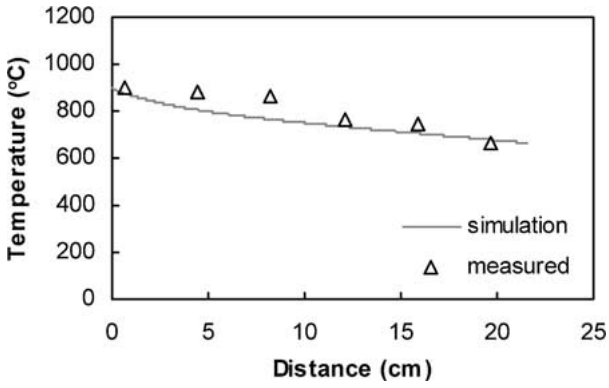


*Figure 11* Metal front temperature during mold filling (coated foam pattern).

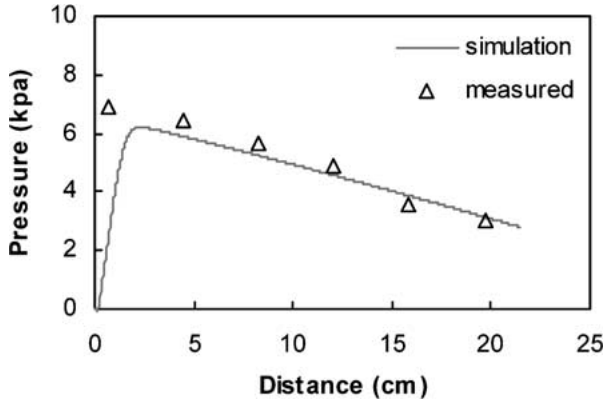


*Figure 12* Internal pressure profile (coated foam pattern).

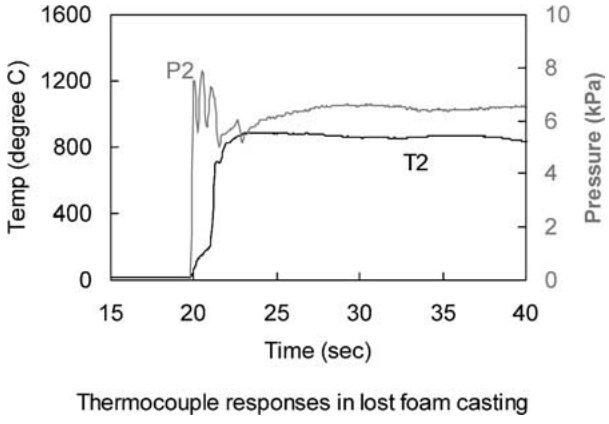


*Figure 13* Typical temperature and pressure profiles.

endothermic. According to Shivkumar *et al*. [15], the energy required for polymer foam degradation is greater than 1 kJ/gram. Because of these endothermic losses at the metal front, steep thermal gradients are generated within the casting. These gradients in the liquid metal even establish directional solidification of the casting [16].

The mold filling velocity shown in Fig. 9 is in the order of 3 cm/s, which is much slower than that for the uncoated pattern. For the aluminum alloys, typical values of the filling velocity for lost foam and empty mold castings are in the order of 10 cm/s and 80–100 cm/s, respectively [17]. In the experiments conducted by Yang *et al*. [5] the mold filling velocity was between 1.6 to 4.6 cm/s.

As the metal front approaches the gas pressure tubes, solid EPS foam experienced series of transitions: collapse, liquidation and finally vaporization. Most of the degradation gaseous species were eliminated through the refractory coating and sequentially dissipated into the sand. The bronze tubes detected the gas pressure evolution inside the foam pattern during mold filling. Fig. 13 shows typical temperature and pressure profiles during casting. Initially, pressure tested by the gas transducers was zero. Once the metal front reached the location of the tube, gas pressure inside the mold rises rapidly to almost the maximum value. However, pressure fluctuations were observed during two seconds, before the stable pressure values were finally achieved. The maximum pressure achieved was 6.59 kPa and the minimum gas pressure was 3.1 kPa. The pressure values presented here are well agree with data obtained by Zhu *et al*. [7].

## 5. Conclusions

A predictive mathematical model was developed and solved for lost foam casting process involving transient heat and mass transfer, and chemical reaction phenomena. The method of Crank-Nicholson was used to reduce the partial differential equations to the algebraic equations, and the Gauss-Seidel iteration used to solve them. Mold filling velocity, temperature distribution, and internal pressures were predicted and compared to the experimentally determined data. The experiments using both coated and uncoated foam patterns were conducted to examine the numerical model. It was found that the model is able to predict all the above casting parameters in close agreement with the measured data. A gas pressure could reach 6.57 kPa in aluminum casting, which agrees with some data reported in the literature.

## Acknowledgements

The authors gratefully acknowledge the financial support received from NASA's Office of Space Access and Technology under Grant No. NAGW-1192. We wish to thank engineering and technical staff of Citation Foam Casting Company, Columbiana, AL for preliminary discussions on the problem of the lost foam casting process. We wish to thank Mr. Don Sirois and Mr. Kayce Weakley for technical assistance in design and fabrication of the experimental apparatus, Mr. Mike Crumpler for writing a program for thermometric measurements.

## References

1. M. J. LESSITER, *Modern Casting* **4** (1997) 32.
2. L. WANG, S. SHIVKUMAR and D. APELIAN, *AFS Transactions* **181** (1990) 923.
3. Y. SUN, H. L. TSAI and D. R. ASKELAND, *ibid.* **104** (1996) 271.
4. S. SHIVKUMAR, X. YAO and M. MAKHLOUF, *Scripta Metallurgica et Materialia* **33** (1995) 39.
5. J. YANG, T. HUANG and J. FU, *AFS Transactions* **128** (1998) 21.
6. T. SHIH and A. CHANG, *ibid.* **110** (1997) 387.
7. J. ZHU, I. OHNAKA, T. OHMICHI, K. MINESHITA and Y. YOSHIOKA, *J. Japan Foundry Engineering Society* **72** (2000) 715.
8. H. L. TSAI and T. S. CHEN, *AFS Transactions* **86** (1988) 881.
9. S. ABAYARATHNA and H. L. TSAI, *ibid.* **130** (1989) 645.
10. S. ABAYARATHNA, *ibid.* **131** (1989) 653.
11. I. OHNAKA, in "Modeling of Casting, Welding and Advanced Solidification Processes VI," edited by T. S. Piwonka *et al.* (MMMS, 1993) p. 337.
12. C. M. WANG, A. J. PAUL and O. J. HUEY, in "Modeling of Casting, Welding and Advanced Solidification Processes VI," edited by T. S. Piwonka *et al*. (MMMS, 1993) 477.
13. W.-S. HWANG, *Advanced Casting Technology* **2** (1986) 71.
14. M. N. OZISIK, "Finite Difference Methods in Heat Transfer" (CRC Press, Florida, 1994).
15. S. SHIVKUMAR, L. WANG and D. APELIAN, *JOM* **38** (1990) 38.
16. M. C. FLEMMINGS, *British Foundryman* **57** (1964) 312.
17. M. H. WARNER, B. A. MILLER and H. E. LITTLETON, *AFS Transactions* **161** (1998) 77.

*Received 23 April 2001*
*and accepted 29 March 2002*